

# Higgs Production in Association with a Dark- $Z$ at Future Electron Positron Colliders

Pierce Giffin,<sup>1,2,\*</sup> Ian M. Lewis,<sup>1,†</sup> and Ya-Juan Zheng<sup>1,‡</sup>

<sup>1</sup>*Department of Physics and Astronomy,*

*University of Kansas, Lawrence, Kansas 66045 U.S.A.*

<sup>2</sup>*Department of Physics, University of California, Santa Cruz, CA 95064, USA*

## Abstract

In recent years there have been many proposals for new electron-positron colliders, such as the Circular Electron-Positron Collider, the International Linear Collider, and the Future Circular Collider in electron-positron mode. Much of the motivation for these colliders is precision measurements of the Higgs boson and searches for new electroweak states. Hence, many of these studies are focused on energies above the  $hZ$  threshold. However, there are proposals to run these colliders at the lower  $WW$  threshold and  $Z$ -pole energies. In this paper, we propose a new search for Higgs physics accessible at lower energies:  $e^+e^- \rightarrow hZ_d$ , where  $Z_d$  is a new light gauge boson such as a dark photon or dark- $Z$ . Such searches can be conducted at the  $WW$  threshold, i.e. energies below the  $hZ$  threshold where exotic Higgs decays can be searched for in earnest. Additionally, due to very good angular and energy resolution at future electron-positron colliders, these searches will be sensitive to  $Z_d$  masses below 1 GeV, which is lower than the current direct LHC searches. We will show that at  $\sqrt{s} = 160$  GeV with  $10 \text{ ab}^{-1}$ , a search for  $e^+e^- \rightarrow hZ_d$  is sensitive to  $h - Z - Z_d$  couplings of  $\delta \sim 8 \times 10^{-3}$  and cross sections of  $\sim 1 - 2 \text{ ab}$  for  $Z_d$  masses below 1 GeV. The results are similar at  $\sqrt{s} = 240$  GeV with  $5 \text{ ab}^{-1}$ .

---

\*Electronic address: pgiffin@ucsc.edu

†Electronic address: ian.lewis@ku.edu

‡Electronic address: yjzheng@ku.edu

## I. INTRODUCTION

A central aspect to many of the proposals for future high energy colliders after the LHC is the prospect of discovering new physics associated with the Higgs boson [1–5]. The high luminosity and clean environments of future electron-positron colliders make them particularly well suited to searches for new physics in precision measurements of the SM Higgs [6–18] and new electroweak (EW) physics in general. Most of these studies of Higgs searches and measurements have been focused on energies at or above 240-250 GeV, which are the energies appropriate for EW production of the 125 GeV Higgs boson in the SM. Indeed, there has been much work on discovering new states associated with the Higgs boson at these energies [19–21].

However, many proposed lepton colliders such as the Circular Electron Positron Collider (CEPC) [22, 23], International Linear Collider (ILC) [24–26], and Future Circular Collider in electron-positron mode (FCC-ee) [27] also propose to conduct precision measurements of EW parameters with runs at the  $Z$ -pole and/or  $WW$ -threshold. In this paper, we propose a novel search involving the 125 GeV Higgs boson that can be carried out at energies below 240 GeV: Higgs production in association with a new light gauge boson.

Many models have the Higgs boson ( $h$ ) as a portal to a dark sector with couplings to a gauge boson of a broken  $U(1)$  symmetry. Such gauge bosons are theoretically well-motivated (see Ref. [28–33] and references therein) and are the so-called “dark photons” [34–37] or “dark- $Z$ s” [38–40]. If the new gauge boson ( $Z_d$ ) is light enough the Higgs boson can decay into it:  $h \rightarrow Z Z_d$  [39–43] and  $h \rightarrow Z_d Z_d$  [42–44]. The same interaction that facilitates the  $h \rightarrow Z Z_d$  decay can also facilitate Higgs production in association with the  $Z_d$ :  $f\bar{f} \rightarrow Z^* \rightarrow h Z_d$ . In this paper we will show that  $e^+e^- \rightarrow Z^* \rightarrow h Z_d$  is possibly discoverable at future electron-positron colliders. There are two interesting points to make about this search:

1. If the  $Z_d$  is light,  $e^+e^- \rightarrow h Z_d$  can be searched for at colliders with energies below 240 GeV. Indeed, we will show that this process is discoverable at a 160 GeV machine with  $10 \text{ ab}^{-1}$  of data [27], i.e. the  $WW$  threshold. Hence, it is possible to search for exotic  $h - Z - Z_d$  couplings below energies for which the Higgs can be produced via the traditional mode  $e^+e^- \rightarrow h Z$ , at which point exotic Higgs decays can be searched for in earnest.

2. As we also will show, due to the very good energy and angular resolutions, for leptonic  $Z_d \rightarrow \ell^+\ell^-$  decays it will be possible to discover a dark- $Z$  with mass below 1 GeV,  $m_{Z_d} \lesssim 1$  GeV, via its interactions with the Higgs. Current LHC searches for  $h \rightarrow Z Z_d$  and  $h \rightarrow Z_d Z_d$  are limited to masses above 1 GeV [45, 46]. Hence, this search at a future electron-positron collider has the potential to open up new regions of parameter space.

The paper is organized as follows. In Sec. II we introduce the model and give an overview of current constraints on model parameters. We present our collider analysis in Sec. III. The results of our study are given in Sec. IV. Finally, in Sec. V we conclude.

## II. MODEL AND CONSTRAINTS

We consider a massive vector boson,  $Z_d$ , originating from a broken  $U(1)_d$  and assume the SM fermions are not charged under this  $U(1)_d$ . Hence, the Higgs will serve as the portal between a dark sector and the SM. We will consider interactions after  $SU(2)_L \times U(1)_Y$  breaking. There are two scenarios of interest for us, when the  $Z_d$  is a dark photon [34–37] or dark- $Z$  [38–40]. In the dark photon scenario, the  $Z_d$  kinetically mixes with the SM hypercharge. This scenario has garnered much attention in the literature and there have been many searches at low energy, high intensity experiments [32, 33]. The kinetic mixing is often thought of as arising via loops of particles charged under both the SM hypercharge and the  $U(1)_d$  symmetry. If the particles inside the loops couple to the Higgs boson, these loops can also induce effective interactions between the Higgs and dark-photon [47]:<sup>1</sup>

$$\mathcal{O}_{B,X} = \frac{c_{B,X}}{\Lambda} h X_{\mu\nu} Z_d^{\mu\nu}, \quad \text{where } X = Z, \gamma, Z_d, \quad (1)$$

and  $\Lambda$  is a new physics scale. An alternative is the dark- $Z$  scenario [38–40] when the SM  $Z$  and the  $Z_d$  have mass mixing. This case typically has a different coupling pattern to fermions than the dark photon, and can indeed induce new sources of parity violation [38, 40]. In this case the couplings with the Higgs are expected to occur at dimension 3:

$$\mathcal{O}_{A,X} = c_{A,X} h X_\mu Z_d^\mu, \quad \text{where } X = Z, Z_d. \quad (2)$$

---

<sup>1</sup> We follow the notation of Ref. [39] for the operators.

Here we cannot have  $X = \gamma$  due to gauge invariance. Interactions such as  $\mathcal{O}_{A,X}$  can also be induced via the mixing of the SM Higgs with the Higgs of a dark sector, see Ref. [44] for an example.

In this paper we propose to search for  $e^+e^- \rightarrow X^* \rightarrow h Z_d$ . Unless the SM is charged under the  $U(1)_d$ , the coupling  $e^+ - e^- - Z_d$  will be suppressed by a mixing angle. Hence, this rate is suppressed for  $X = Z_d$ . If  $X = Z$ , the rate is not suppressed by the initial state coupling. The photon mediated process  $X = \gamma$  is also possible for the operator  $\mathcal{O}_{B,X}$ , but not possible for  $\mathcal{O}_{A,X}$ .

From this discussion, we will consider interactions with  $X = Z$ . Following Refs. [39, 40], we parameterize  $c_{A,Z}$  assuming that  $\mathcal{O}_{A,Z}$  arises from  $Z - Z_d$  mass mixing:

$$c_{A,Z} = \frac{g}{c_W} m_{Z_d} \delta. \quad (3)$$

We will also consider the limit where the mass of the  $Z_d$  is much smaller than other scales in the problem:  $m_{Z_d} \ll m_Z, \sqrt{s}$ , where  $m_Z$  is the  $Z$  mass and  $\sqrt{s}$  is center of momentum frame energy. The production rate when only  $\mathcal{O}_{A,Z}$  contributes is

$$\sigma_A(s) = \frac{g^4 \delta^2}{384 \pi c_W^4} (g_L^2 + g_R^2) \frac{1}{s} \left(1 - \frac{m_h^2}{s}\right)^3 \left(1 - \frac{m_Z^2}{s}\right)^{-2} + \mathcal{O}\left(\frac{m_{Z_d}^2}{s^2}\right) \quad (4)$$

whereas the rate when only  $\mathcal{O}_{B,Z}$  contributes is

$$\sigma_B(s) = \frac{g^2 c_{B,Z}^2}{48 \pi c_W^2 \Lambda^2} (g_L^2 + g_R^2) \left(1 - \frac{m_h^2}{s}\right)^3 \left(1 - \frac{m_Z^2}{s}\right)^{-2} + \mathcal{O}\left(\frac{m_{Z_d}^2}{s \Lambda^2}\right), \quad (5)$$

where  $m_h = 125$  GeV is the Higgs boson mass,  $g_L = s_W^2$  and the  $g_R = -1/2 + s_W^2$  are the left- and right-chiral electron- $Z$  couplings, and  $c_W = \cos \theta_W$ ,  $s_W = \sin \theta_W$  with  $\theta_W$  being the weak mixing angle. As can be seen the energy dependence of  $\sigma_A(s)$  and  $\sigma_B(s)$  is different, due to the fact that  $\mathcal{O}_{A,Z}$  is a dimension-3 operator while  $\mathcal{O}_{B,Z}$  is a non-renormalizable dimension-5 operator. In Fig. 1 we show the  $e^+e^- \rightarrow h Z_d$  cross section for both  $\delta = 0$  and  $c_{B,Z} = 0$ . The dimension-5 cross section asymptotes to a constant value at high energy, while the cross section from  $\mathcal{O}_{A,Z}$  peaks at  $\sqrt{s} \sim 220$  GeV and then decreases as energy increases.

An interesting feature of this is that ratios of cross sections at different energies can help shed light on the origin of the  $h - Z - Z_d$  interaction. Considering  $\sqrt{s} = 160$  and 240 GeV, the ratio of rates for  $c_{B,Z} = 0$  and  $\delta = 0$  are

$$\frac{\sigma_A(s = (160 \text{ GeV})^2)}{\sigma_A(s = (240 \text{ GeV})^2)} = 0.55 \quad \text{and} \quad \frac{\sigma_B(s = (160 \text{ GeV})^2)}{\sigma_B(s = (240 \text{ GeV})^2)} = 0.25, \quad (6)$$

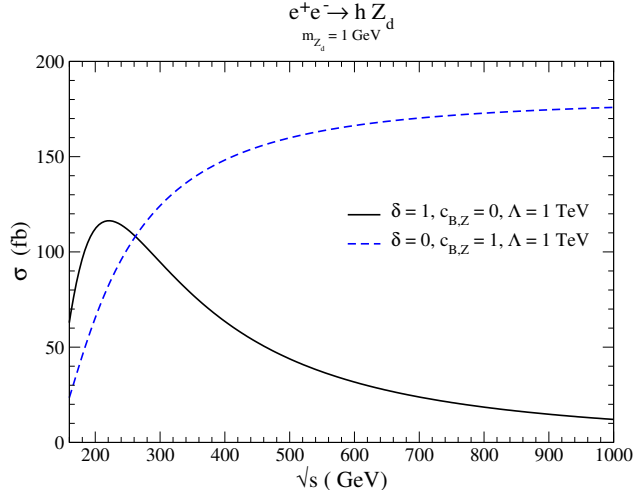


FIG. 1: Production cross section for  $e^+e^- \rightarrow h Z_d$  as a function of center of momentum energy  $\sqrt{s}$  with (black solid)  $\delta = 1$ ,  $c_{B,Z} = 0$  and (blue dashed)  $\delta = 0$ ,  $c_{B,Z} = 1$ . For both curves  $m_{Z_d} = 1$  GeV and  $\Lambda = 1$  TeV.

respectively. As we go out to ever higher energies this effect becomes more pronounced.

As mentioned earlier, typical direct LHC searches for  $h \rightarrow Z Z_d$  are for  $m_{Z_d} \gtrsim 1$  GeV [45, 46]. Hence, their constraints are not relevant for our parameter space of  $m_{Z_d} \lesssim 1$  GeV. However, for these light masses there are still many relevant lower energy searches and precision measurements [33]. The bounds from these searches are usually reported in the dark-photon parameter space. For  $m_{Z_d}$  in the 0.1 – 1 GeV mass range, the dark photon mixing parameter is limited to be less than  $\sim 10^{-3}$ . If the  $Z_d$  is light enough it can contribute to exotic meson decays  $K \rightarrow \pi Z_d$  [48] and  $B \rightarrow K Z_d$  [40], both of which place limits  $|\delta| \lesssim 10^{-3}$ . There are a few caveats to these bounds. First, there can be cancellations between the kinetic and mass mixings that can alleviate some of these bounds [48]. Additionally, many of these constraints are on the SM fermion and gauge boson couplings to the  $Z_d$ . The connection between the fermion- $Z_d$  couplings and  $c_{A,Z}, c_{B,Z}$  will depend precisely on the UV complete model and the origin of  $\mathcal{O}_{A,Z}$  and  $\mathcal{O}_{B,Z}$ . Due to this, it is interesting to independently search for processes that arise out of the  $h - Z - Z_d$  couplings, even if the parameter space appears to be constrained.

There are additional limits from the LHC that bound the  $h - Z - Z_d$  coupling. Using measurements of the Higgs production and decay modes via SM particles, it is possible to place limits on the Higgs branching ratio to undetected final states,  $\text{BR}_{\text{BSM}}$ , with minimal

assumptions [49]. These bounds are relevant for  $h \rightarrow Z Z_d$  independent of dedicated searches. Assuming no other new physics decay modes or modifications to couplings, the branching ratio into  $h \rightarrow Z Z_d$  is

$$\text{BR}(h \rightarrow Z Z_d) = \frac{\Gamma(h \rightarrow Z Z_d)}{\Gamma_{\text{SM}} + \Gamma(h \rightarrow Z Z_d)}, \quad (7)$$

where  $\Gamma_{\text{SM}} = 4.088 \text{ MeV}$  is the total width into SM final states [50]. Assuming  $m_{Z_d} \ll m_h$  the partial width with  $c_{B,Z} = 0$  is

$$\Gamma(h \rightarrow Z Z_d) = \frac{g^2 \delta^2}{64 \pi c_W^2} \frac{m_h^3}{m_Z^2} \left(1 - \frac{m_Z^2}{m_h^2}\right)^3 \quad (8)$$

and if  $\delta = 0$  the partial width is

$$\Gamma(h \rightarrow Z Z_d) = \frac{1}{8\pi} \left(\frac{c_{B,Z}}{\Lambda}\right)^2 m_h^3 \left(1 - \frac{m_Z^2}{m_h^2}\right)^3. \quad (9)$$

At the HL-LHC the projected limit is  $\text{BR}_{\text{BSM}} \leq 0.025$  [3]. This translates to a bound  $|\delta| \leq 0.04$  or  $|c_{B,Z}/\Lambda| \leq 0.11 \text{ TeV}^{-1}$ . As we will show, searches for the direct production  $e^+e^- \rightarrow h Z_d$  are more sensitive to the  $h - Z - Z_d$  coupling.

### III. COLLIDER ANALYSIS

We study the process  $e^+e^- \rightarrow Z^* \rightarrow h Z_d$  at the energies  $\sqrt{s} = 160 \text{ GeV}$  and  $240 \text{ GeV}$ . For simplicity, in our collider analysis we will assume only  $\mathcal{O}_{A,Z}$  contributes and set

$$c_{B,Z} = 0. \quad (10)$$

For better signal reconstruction, the leptonic decays of the  $Z_d$  are considered:  $Z_d \rightarrow \ell^+ \ell^-$  with  $\ell = e, \mu$ . To increase rates, we consider the hadronic decays of the Higgs:  $h \rightarrow b\bar{b}, gg, c\bar{c}$ . `Madgraph5_aMC@NLO` [51] is used for all event generation with the interaction  $\mathcal{O}_{A,Z}$  implemented via `FeynRules` [52, 53]. The Higgs branching ratios are normalized to agree with the LHC Higgs Cross Section Working Group [50]. Production and decays are simulated at parton level, then detector effects are modeled by Gaussian smearing of the energies and momentum of final state particles. Final state quarks and gluons are smeared according to the hadronic calorimeter energy resolution [23, 27]:

$$\frac{\Delta E}{E} = \frac{0.34}{\sqrt{E/\text{GeV}}}. \quad (11)$$

The electron and muon energies are smeared according to the tracking system momentum resolution [23, 27]:

$$\Delta \left( \frac{1}{p_T} \right) = 2 \times 10^{-5} \text{ GeV}^{-1} \otimes \frac{10^{-3}}{p_T \sqrt{\sin \theta}}. \quad (12)$$

We adopt the following pre-selection acceptance cuts:

$$\begin{aligned} p_{T,j} > 20 \text{ GeV}, \quad p_{T,\ell} > 0.5 \text{ GeV} \\ |\cos \theta_{\ell,j}| < 0.98, \quad \Delta R_{ij} > 0.005, \quad p_{T,\ell\ell} > 20 \text{ GeV}, \end{aligned} \quad (13)$$

where  $p_{T,j}, p_{T,\ell}$  are jet and lepton transverse momentum,  $\theta_{\ell,j}$  are the lepton and jet polar angles in the detector,  $\Delta R_{ij} = \sqrt{(\Delta\phi_{ij})^2 + (\Delta\eta_{ij})^2}$  with  $\Delta\phi_{ij}$  ( $\Delta\eta_{ij}$ ) the azimuthal angle (rapidity) difference between particles  $i$  and  $j$ , and  $p_{T,\ell\ell}$  is the di-lepton transverse momentum. For all numerical results presented in this section, we consider the signal parameter points:

$$\delta \times \sqrt{\text{BR}(Z_d \rightarrow \ell^+\ell^-)} = 1.5 \times 10^{-2} \quad \text{with} \quad m_{Z_d} = 0.5 \text{ and } 1 \text{ GeV}, \quad (14)$$

where  $\text{BR}(Z_d \rightarrow \ell^+\ell^-) = \text{BR}(Z_d \rightarrow \mu^+\mu^-) + \text{BR}(Z_d \rightarrow e^+e^-)$ .

For the background process, we include all the channels, except  $h\ell^+\ell^-$ , which can produce  $\ell^+\ell^-jj$  and fully take into consideration the interference between the different SM background processes. The background  $h\ell^+\ell^-$  is considered separately at  $\sqrt{s} = 240$  GeV due to the very small Higgs width. In Figs. 2 and 3 we show the normalized distributions of signal and background cross sections at  $\sqrt{s} = 160$  GeV and 240 GeV, respectively. Clearly, the signal has very different behavior than the background. The high energy and angular resolution of future lepton-colliders can help significantly to separate signal from background. The angular resolution is expected to be better than  $10^{-3}$  and the energy resolution for a lepton with energy below 100 GeV is  $\lesssim 1\%$  [23, 27]. Hence, from these figures it is clear that the decay products of the  $Z_d$  are resolvable and the  $Z_d$  mass is reconstructable even for  $m_{Z_d} \lesssim 1$  GeV.

Signal versus background discrimination also benefits from the signal being a two-to-two process, while the background in the signal region is at best two-to-three. From the  $e^+e^- \rightarrow h Z_d$  kinematics, the energy of the  $Z_d$  is expected to be

$$E_{Z_d} = \frac{s + m_{Z_d}^2 - m_h^2}{2\sqrt{s}}. \quad (15)$$

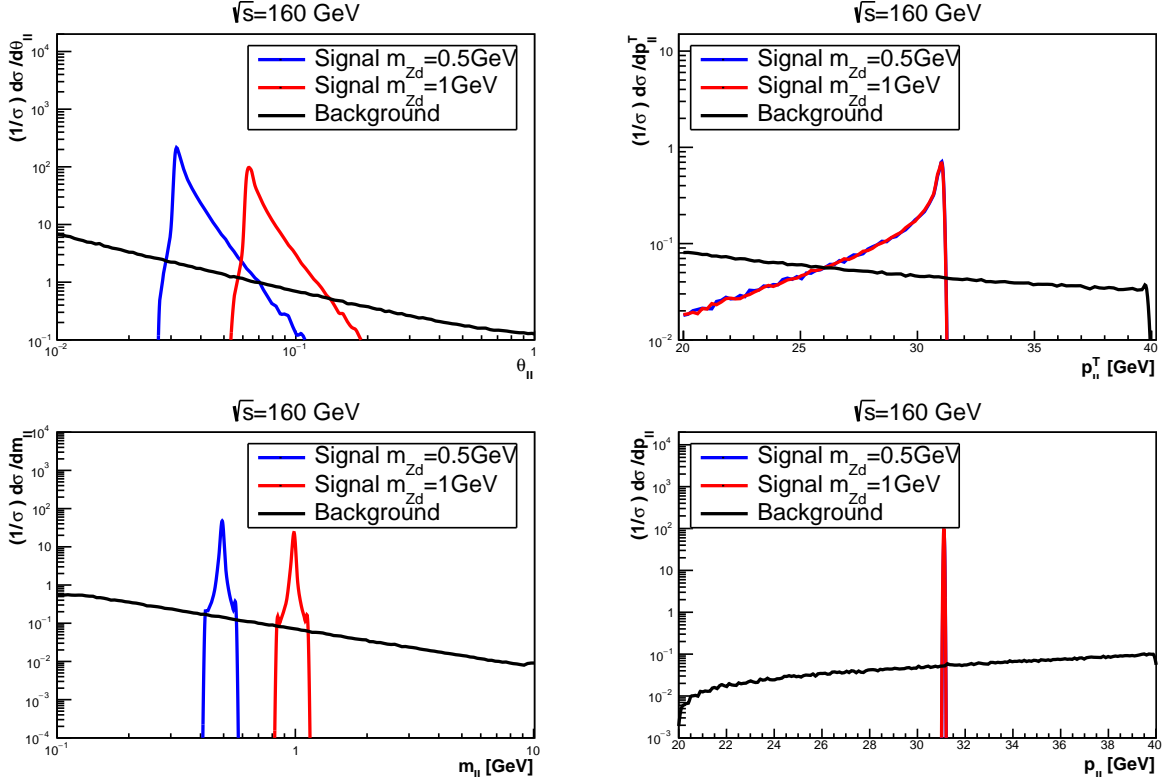


FIG. 2: Normalized distributions of the di-lepton (upper left) opening angle  $\theta_{\ell\ell}$ , (upper right) transverse momentum  $p_{T,\ell\ell}$ , (lower left) invariant mass  $m_{\ell\ell}$ , and (lower right) 3-momentum magnitude  $|\vec{p}|_{\ell\ell}$  for (black) the  $\ell^+\ell^-jj$  background, (red) the signal with  $m_{Z_d} = 1$  GeV, and (blue) the signal with  $m_{Z_d} = 0.5$  GeV. These are at  $\sqrt{s} = 160$  GeV.

For  $m_{Z_d} \lesssim 1$  GeV, the  $Z_d$  mass can be neglected and the magnitude of the  $Z_d$  three-momentum is

$$|\vec{p}_{Z_d}| = \begin{cases} 31 \text{ GeV} & \text{for } \sqrt{s} = 160 \text{ GeV} \\ 87 \text{ GeV} & \text{for } \sqrt{s} = 240 \text{ GeV} \end{cases}. \quad (16)$$

This is precisely where the signal di-lepton three-momentum and transverse momentum peak in Figs. 2 and 3.

Based on these considerations, we adopt the following cuts. At  $\sqrt{s} = 160$  GeV, we require

$$\begin{aligned} 30.5 \text{ GeV} < |\vec{p}|_{\ell\ell} < 31.5 \text{ GeV}, & \quad (17) \\ 25 \text{ GeV} < p_{T,\ell\ell} < 31.5 \text{ GeV}, & \\ 0.051 < \theta_{\ell\ell} < 0.2 \text{ for } m_{Z_d} = 1 \text{ GeV}, & \quad 0.03 < \theta_{\ell\ell} < 0.1 \text{ for } m_{Z_d} = 0.5 \text{ GeV}, \\ 0.8 < m_{\ell\ell}/\text{GeV} < 1.25 \text{ for } m_{Z_d} = 1 \text{ GeV}, & \quad 0.4 < m_{\ell\ell}/\text{GeV} < 0.6 \text{ for } m_{Z_d} = 0.5 \text{ GeV}. \end{aligned}$$



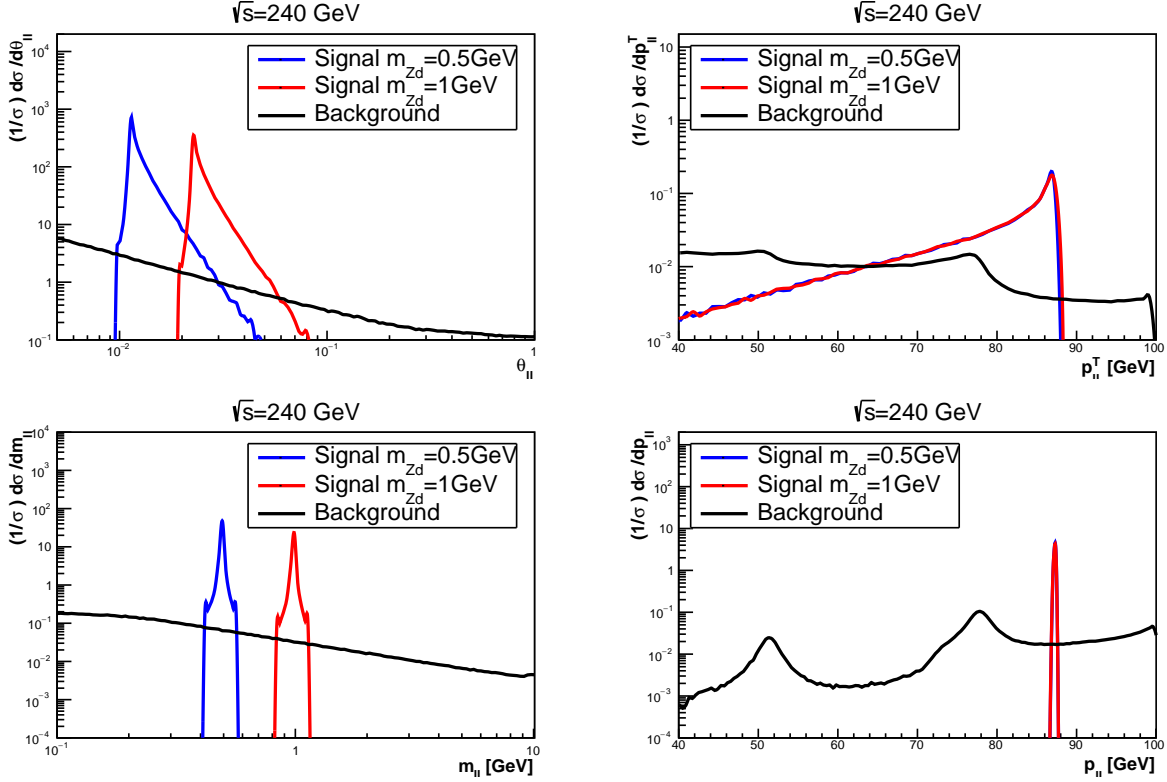


FIG. 3: Same as Fig. 2 with  $\sqrt{s} = 240$  GeV.

At  $\sqrt{s} = 240$  GeV, we require

$$\begin{aligned}
 85 \text{ GeV} < |\vec{p}|_{\ell\ell} < 90 \text{ GeV}, \\
 60 \text{ GeV} < p_{T,\ell\ell} < 90 \text{ GeV},
 \end{aligned}
 \tag{18}$$

$$\begin{aligned}
 0.018 < \theta_{\ell\ell} < 0.089 \text{ for } m_{Z_d} = 1 \text{ GeV}, & \quad 0.009 < \theta_{\ell\ell} < 0.045 \text{ for } m_{Z_d} = 0.5 \text{ GeV}, \\
 0.75 < m_{\ell\ell}/\text{GeV} < 1.25 \text{ for } m_{Z_d} = 1 \text{ GeV}, & \quad 0.25 < m_{\ell\ell}/\text{GeV} < 0.75 \text{ for } m_{Z_d} = 0.5 \text{ GeV}.
 \end{aligned}$$

Since the signal also contains the hadronic decays of a Higgs boson, we require the di-jet invariant mass to pass the cut<sup>2</sup>

$$115 \text{ GeV} < m_{jj} < 135 \text{ GeV},
 \tag{19}$$

at both 160 and 240 GeV.

In Table I we show our cut flows for our benchmark signal points and background at both  $\sqrt{s} = 160$  and 240 GeV. Here we include the  $h \ell^+ \ell^-$  backgrounds at 240 GeV. There are

<sup>2</sup> It may be possible to reconstruct the Higgs recoil mass from the reconstructed  $Z_d$  and place a tighter cut.

Cross Sections		$\sqrt{s} = 160 \text{ GeV}$		$\sqrt{s} = 240 \text{ GeV}$		
$m_{Z_d}$	Cut Flow	Signal	Background $\ell\ell jj$	Signal	Background	
					$\ell\ell jj$	$h\ell^+\ell^-$
0.5 GeV	Pre-selection	8.8 ab	$7.6 \times 10^5$ ab	16 ab	$7.4 \times 10^5$ ab	$1.0 \times 10^4$ ab
	+ $m_{jj}$ cut	8.2 ab	$2.1 \times 10^4$ ab	15 ab	$1.2 \times 10^4$ ab	$9.7 \times 10^3$ ab
	+ $ \vec{p} _{\ell\ell}$ cut	8.2 ab	$1.2 \times 10^3$ ab	15 ab	$2.6 \times 10^3$ ab	5.2 ab
	+ $p_{T,\ell\ell}$ cut	6.4 ab	290 ab	13 ab	370 ab	3.3 ab
	+ $\theta_{\ell\ell}$ cut	6.4 ab	62 ab	13 ab	100 ab	$7.9 \times 10^{-3}$ ab
	+ $m_{\ell\ell}$ cut	6.4 ab	18 ab	13 ab	55 ab	$1.4 \times 10^{-3}$ ab
1 GeV	Pre-selection	8.8 ab	$7.6 \times 10^5$ ab	16 ab	$7.4 \times 10^5$ ab	$1.0 \times 10^4$ ab
	+ $m_{jj}$ cut	8.2 ab	$2.1 \times 10^4$ ab	15 ab	$1.2 \times 10^4$ ab	$9.7 \times 10^3$ ab
	+ $ \vec{p} _{\ell\ell}$ cut	8.2 ab	$1.2 \times 10^3$ ab	15 ab	$2.6 \times 10^3$ ab	5.2 ab
	+ $p_{T,\ell\ell}$ cut	6.4 ab	290 ab	13 ab	370 ab	3.3 ab
	+ $\theta_{\ell\ell}$ cut	6.4 ab	69 ab	13 ab	100 ab	$4.1 \times 10^{-2}$ ab
	+ $m_{\ell\ell}$ cut	6.4 ab	21 ab	13 ab	28 ab	$2.6 \times 10^{-3}$ ab

TABLE I: Cut flow table for both  $\sqrt{s} = 160$  and  $240$  GeV for our benchmark point  $\delta \times \sqrt{\text{BR}(Z_d \rightarrow \ell\ell)} = 1.5 \times 10^{-2}$ . Here  $\text{BR}(Z_d \rightarrow \ell^+\ell^-) = \text{BR}(Z_d \rightarrow e^-e^+) + \text{BR}(Z_d \rightarrow \mu^-\mu^+)$ .

also  $\tau\tau jj$  backgrounds with leptonic  $\tau$  decays, but they are sub-leading due to the small  $\tau$  leptonic branching ratios and the fact that these backgrounds could be further suppressed with missing energy cuts. As can be seen, our cuts have small effect on our signal acceptance, with an efficiency of 72 – 82%, but are very efficient at suppressing background. Cuts on the di-jet invariant mass suppress non-Higgs backgrounds by over an order of magnitude. The di-lepton 3-momentum and transverse momentum cuts suppress the background by nearly another order of magnitude. The di-lepton opening angle and invariant mass cuts suppress the background by yet another order of magnitude. Hence, even though background starts out at more than four orders of magnitude larger than signal, after cuts the signal to background ratio is a manageable  $S/B \sim 0.2 - 0.5$ .

$\sqrt{s}$	Luminosity	$m_{Z_d}$	no b-tag			1 b-tag		
			Signal	Background	$\sigma_{\text{disc}}$	Signal	Background	$\sigma_{\text{disc}}$
160 GeV	10 $\text{ab}^{-1}$	0.5 GeV	64	180	4.6	43	23	7.3
		1 GeV	64	210	4.2	43	28	6.8
240 GeV	5 $\text{ab}^{-1}$	0.5 GeV	67	280	3.9	46	43	6.1
		1 GeV	67	140	5.3	46	22	7.7

TABLE II: Number of signal and background events, and discovery significance [Eq. (21)] at both  $\sqrt{s} = 160$  and 240 GeV with benchmark luminosities 10 and 5  $\text{ab}^{-1}$ , respectively. Results shown for benchmarks  $\delta \times \sqrt{\text{BR}(Z_d \rightarrow \ell^+ \ell^-)} = 1.5 \times 10^{-2}$  and  $m_{Z_d} = 0.5$  and 1 GeV. Here  $\text{BR}(Z_d \rightarrow \ell^+ \ell^-) = \text{BR}(Z_d \rightarrow e^- e^+) + \text{BR}(Z_d \rightarrow \mu^- \mu^+)$ .

#### IV. RESULTS

We now present the results of our analysis, and estimate the reaches of future electron-positron colliders. In Table II, we show the estimated number of signal and background events as well as the discovery significance at 160 GeV with 10  $\text{ab}^{-1}$  and 240 GeV with 5  $\text{ab}^{-1}$ , which are the design luminosities of the FCC-ee [27]. Using a Poisson likelihood

$$L(x|n) = \frac{x^n}{n!} e^{-x}, \quad (20)$$

for a given number of signal events  $S$  and background events  $B$ , the significance for discovery is given by the likelihood ratio [54]

$$\sigma_{\text{disc}} = \sqrt{-2 \ln \left( \frac{L(B|B+S)}{L(S+B|S+B)} \right)} = \sqrt{2 \left( (B+S) \log \left( 1 + \frac{S}{B} \right) - S \right)}. \quad (21)$$

That is, discovery is defined as when the background only hypothesis is disfavored at 5-sigma,  $\sigma_{\text{disc}} \geq 5$ , relative to the background plus signal hypothesis.

We also show the results if we require that at least one jet is tagged as a  $b$ -jet. The  $b$ -tagging rate is set to 80%, with a 1% rate for light jets mis-tagged as  $b$ -jets and a 10% mis-tagging rates for charm quarks [23]. Requiring one  $b$ -jet increases the significance since the signal is mostly composed of  $h \rightarrow b\bar{b}$  and the background has many processes with light and charm jets. Since all signal and background processes are flavor conserving, requiring an additional  $b$ -tagged jet suppresses signal and background at similar rates. We found that requiring two  $b$ -tagged jets does not help the significance.

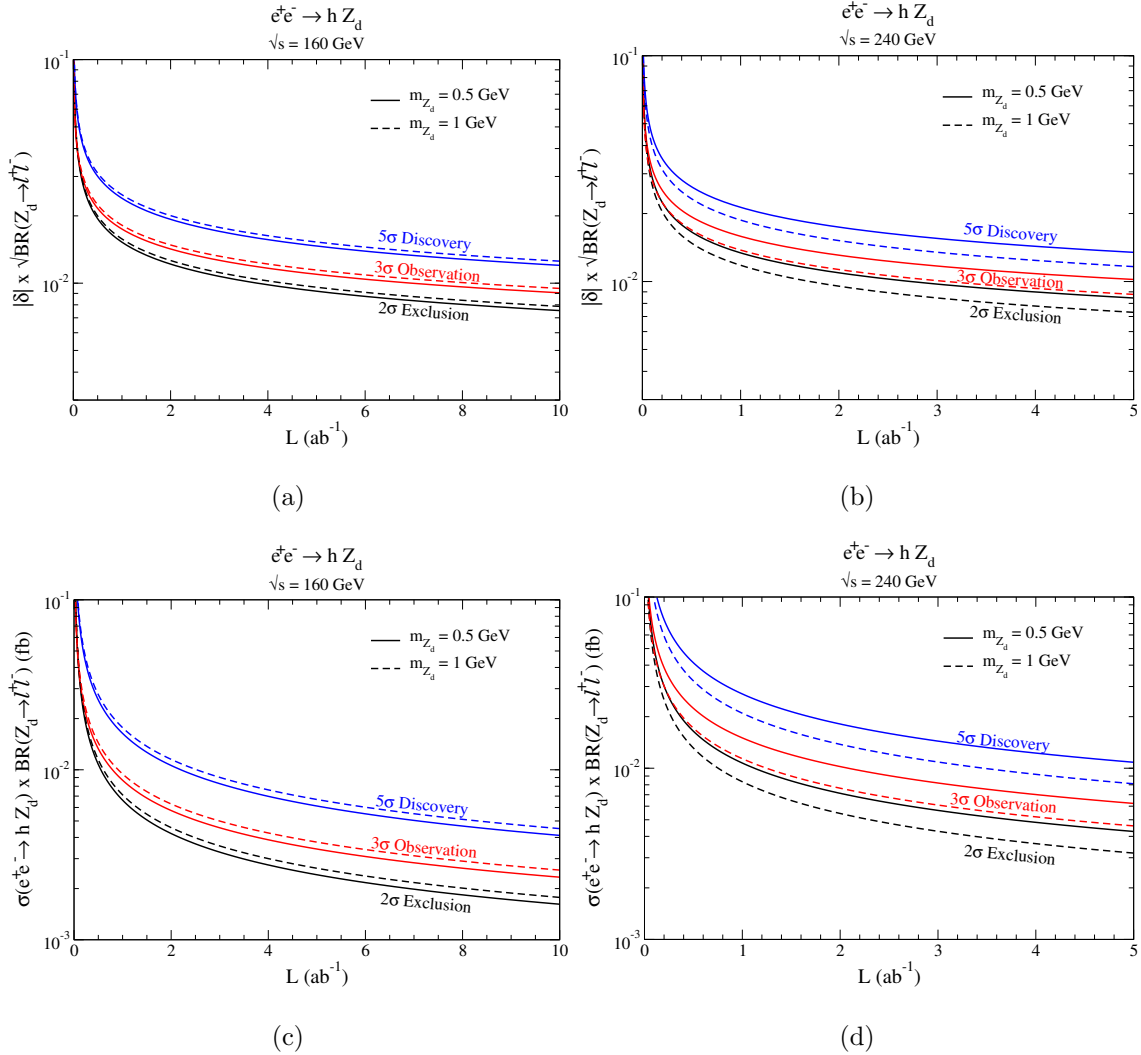


FIG. 4: The luminosity needed for (black) exclusion [Eq. (22)], (red) observation [Eq. (21)], and (blue) discovery [Eq. (21)] for either a given model parameter (a,b)  $\delta \times \sqrt{\text{BR}(Z_d \rightarrow \ell^+ \ell^-)}$  or (c,d) cross section  $\sigma(e^- e^+ \rightarrow h Z_d) \text{BR}(Z_d \rightarrow \ell^+ \ell^-)$ . These are shown at both (a,c)  $\sqrt{s} = 160$  GeV and (b,d)  $\sqrt{s} = 240$  GeV, and for  $Z_d$  masses (solid)  $m_{Z_d} = 0.5$  GeV and (dashed) 1 GeV. At least one  $b$ -tagged jet is required. Here  $\text{BR}(Z_d \rightarrow \ell^+ \ell^-) = \text{BR}(Z_d \rightarrow e^- e^+) + \text{BR}(Z_d \rightarrow \mu^- \mu^+)$ .

In Fig. 4 we show the estimated parameter regions that can be excluded at  $2\sigma$ , observed at  $3\sigma$ , and discovered at  $5\sigma$ . Regions above the curves can be excluded, observed, or discovered. These are found requiring at least one  $b$ -tagged jet. Discovery and observation capability are defined using the discovery significances  $\sigma_{\text{disc}} \geq 5$  and  $\sigma_{\text{disc}} \geq 3$ , respectively. To exclude,

$\sqrt{s}$	Luminosity	$m_{Z_d}$	$ \delta  \times \sqrt{\text{BR}(Z_d \rightarrow \ell^+\ell^-)}$			$\sigma(e^-e^+ \rightarrow h Z_d)\text{BR}(Z_d \rightarrow \ell^+\ell^-)$		
			2 $\sigma$ Exc.	3 $\sigma$ Obs.	5 $\sigma$ Disc.	2 $\sigma$ Exc.	3 $\sigma$ Obs.	5 $\sigma$ Disc.
160 GeV	10 $\text{ab}^{-1}$	0.5 GeV	$7.5 \times 10^{-3}$	$9.1 \times 10^{-3}$	$1.2 \times 10^{-2}$	1.6 ab	2.3 ab	4.1 ab
		1 GeV	$7.9 \times 10^{-3}$	$9.5 \times 10^{-3}$	$1.3 \times 10^{-2}$	1.8 ab	2.6 ab	4.5 ab
240 GeV	5 $\text{ab}^{-1}$	0.5 GeV	$8.4 \times 10^{-3}$	$1.0 \times 10^{-2}$	$1.3 \times 10^{-2}$	4.3 ab	6.2 ab	11 ab
		1 GeV	$7.3 \times 10^{-3}$	$8.8 \times 10^{-3}$	$1.2 \times 10^{-2}$	3.2 ab	4.6 ab	8.1 ab

TABLE III: The smallest values of the parameter  $\delta \times \sqrt{\text{BR}(Z_d \rightarrow \ell^+\ell^-)}$  and cross section  $\sigma(e^+e^- \rightarrow h Z_d)\text{BR}(Z_d \rightarrow \ell^+\ell^-)$  that can be excluded at 2 $\sigma$  (Exc.) [Eq. (22)], observed at 3 $\sigma$  (Obs.) [Eq. (21)], or discovered at 5 $\sigma$  (Disc.) [Eq. (21)]. Results are shown for both masses  $m_{Z_d} = 0.5$  GeV and 1 GeV, and at both  $\sqrt{s} = 160$  and 240 GeV with benchmark luminosities 10 and 5  $\text{ab}^{-1}$ , respectively. At least one  $b$ -tagged jet is required and  $\text{BR}(Z_d \rightarrow \ell^+\ell^-) = \text{BR}(Z_d \rightarrow e^-e^+) + \text{BR}(Z_d \rightarrow \mu^-\mu^+)$ .

the signal plus background hypothesis is tested against the background only hypothesis [54]:

$$\sigma_{\text{exc}} = \sqrt{-2 \ln \left( \frac{L(S+B|B)}{L(B|B)} \right)} = \sqrt{2 \left( S - B \log \left( 1 + \frac{S}{B} \right) \right)}. \quad (22)$$

A signal is excluded at 2 $\sigma$  when  $\sigma_{\text{exc}} \geq 2$ . Note that Fig. 1 shows that for a fixed  $\delta$ , the cross section of  $e^+e^- \rightarrow h Z_d$  is lower at  $\sqrt{s} = 160$  GeV than at  $\sqrt{s} = 240$  GeV. Hence, even though the parameter space reach is similar at both energies, the  $\sqrt{s} = 160$  GeV machine is sensitive to lower cross sections than  $\sqrt{s} = 240$  GeV.

The exclusion, observation, and discovery limits on model parameters and cross sections are given in Table III. With 10  $\text{ab}^{-1}$  at 160 GeV, an electron-positron machine could probe parameters down to  $\delta \times \sqrt{\text{BR}(Z_d \rightarrow \ell^+\ell^-)} \sim 8 \times 10^{-3}$  and cross sections  $\sigma(e^+e^- \rightarrow h Z_d)\text{BR}(Z_d \rightarrow \ell^+\ell^-) \sim 1 - 2$  ab. The sensitivity of a 240 GeV machine with 5  $\text{ab}^{-1}$  is similar:  $\delta \times \sqrt{\text{BR}(Z_d \rightarrow \ell^+\ell^-)} \sim 8 \times 10^{-3}$  and cross sections  $\sigma(e^+e^- \rightarrow h Z_d)\text{BR}(Z_d \rightarrow \ell^+\ell^-) \sim 3 - 4$  ab.

## V. CONCLUSIONS

The particle physics community is going through discussions about future colliders beyond the LHC. Many of these colliders have an extensive program to measure and search for

new physics associated with the Higgs boson. Due to the clean environment and large luminosities, electron-positron colliders will be able to measure the Higgs boson to great precision [22–27]. Indeed, the European Strategy Group has endorsed an electron-positron collider as the next step in the global collider program [55].

We propose a new search  $e^+e^- \rightarrow h Z_d$ , where  $Z_d$  is a new light gauge boson. As discussed in Secs. I and II, models with new light gauge bosons are theoretically well-motivated and there has been much effort in searching for these particles at high intensity, low energy experiments. There have also been LHC searches for  $h \rightarrow Z Z_d$ , which arises from the same interactions as  $e^+e^- \rightarrow h Z_d$ . However, as we discussed in Sec. II and III, the high resolutions of future detectors at electron-positron colliders will allow for searches with  $Z_d$  masses below 1 GeV. Current dedicated LHC searches do not probe masses this low [45, 46].

A particularly compelling argument for this search is that  $e^+e^- \rightarrow h Z_d$  can be observed at collider energies below the  $h Z$  threshold. Indeed, many future electron-positron collider proposals include runs at the  $WW$  threshold and our results indicate there could be discoverable new physics processes involving the Higgs boson at those energies. Using the design luminosities of the FCC-ee, we showed that  $e^+e^- \rightarrow h Z_d$  can be sensitive to parameters and cross sections of

$$\begin{aligned} \delta \sim 8 \times 10^{-3} \quad \text{and} \quad \sigma(e^+e^- \rightarrow h Z_d) \sim 1 - 2 \text{ ab} \quad \text{at} \quad \sqrt{s} = 160 \text{ GeV} \text{ with } 10 \text{ ab}^{-1} \\ \delta \sim 8 \times 10^{-3} \quad \text{and} \quad \sigma(e^+e^- \rightarrow h Z_d) \sim 3 - 4 \text{ ab} \quad \text{at} \quad \sqrt{s} = 240 \text{ GeV} \text{ with } 5 \text{ ab}^{-1}. \end{aligned}$$

Once a discovery is made, it will be necessary to determine the origin of the  $h - Z - Z_d$  coupling. As discussed in Sec. II, by comparing the  $e^+e^- \rightarrow h Z_d$  rate at different energies it will be possible to determine if this coupling originates from dimension-5 or dimension-3 operators. Hence, even if  $h \rightarrow Z Z_d$  is discovered first, searching for and measuring  $e^+e^- \rightarrow h Z_d$  can provide important information about the new physics. Additionally, if  $h - Z - Z_d$  originates from the dimension-5 operator the  $Z_d$  will be predominately transversely polarized, and if it originates from the dimension-3 operator the  $Z_d$  will be predominately longitudinally polarized. Hence, the angular distributions of the  $Z_d$  decay products will also help disentangle the origin of these new interactions [39].

Finally, in our analysis we focused on the leptonic decays  $Z_d \rightarrow \ell^+\ell^-$ . This choice was because the events, and therefore the signal, are fully reconstructable. However, it is possible the the dark- $Z$  could decay into invisible particles, such as neutrinos or dark matter when kinematically allowed. It would be interesting to further this study to include invisible  $Z_d$

decays which would result in a Higgs and missing momentum signature even at 160 GeV. This could be promising for several reasons. (1) Even for hadronic decays the Higgs can be reconstructed well since the jet energy uncertainty is  $\sim 4\%$  for Higgs decay products [Eq. (11)]. (2) At electron-positron colliders the complete missing energy and momentum vector are reconstructable. Due to the two-body kinematics of our signal there is a precise prediction for the energy and the magnitude of that missing momentum vector [Eq. (16)]. Hence, it may still be possible efficiently tag signal events and search for invisible  $Z_d$  decays. It may even be feasible to search for higher  $Z_d$  masses in ranges that are beyond the relevance of low energy constraints but still difficult for direct LHC searches due to the missing energy.

### Acknowledgments

IML would like to thank Hooman Davoudiasl for constructive comments on the manuscript and Hye-Sung Lee for encouraging discussions. IML and YZ are supported in part by the U.S. Department of Energy under grant No. de-sc0019474. PG is supported in part by the State of Kansas EPSCoR grant program.

- 
- [1] N. Arkani-Hamed, T. Han, M. Mangano, and L.-T. Wang, *Physics opportunities of a 100 TeV proton–proton collider*, *Phys. Rept.* **652** (2016) 1–49, [arXiv:1511.06495 \[hep-ph\]](#).
  - [2] M. Mangano *et al.*, *Physics at a 100 TeV pp Collider: Standard Model Processes*, *CERN Yellow Rep.* no. 3, (2017) 1–254, [arXiv:1607.01831 \[hep-ph\]](#).
  - [3] M. Cepeda *et al.*, *Report from Working Group 2: Higgs Physics at the HL-LHC and HE-LHC*, *CERN Yellow Rep. Monogr.* **7** (2019) 221–584, [arXiv:1902.00134 \[hep-ph\]](#).
  - [4] J. de Blas *et al.*, *Higgs Boson Studies at Future Particle Colliders*, *JHEP* **01** (2020) 139, [arXiv:1905.03764 \[hep-ph\]](#).
  - [5] R. K. Ellis *et al.*, *Physics Briefing Book: Input for the European Strategy for Particle Physics Update 2020*, [arXiv:1910.11775 \[hep-ex\]](#).
  - [6] P. Bechtle, S. Heinemeyer, O. Stål, T. Stefaniak, and G. Weiglein, *Probing the Standard Model with Higgs signal rates from the Tevatron, the LHC and a future ILC*, *JHEP* **11** (2014) 039, [arXiv:1403.1582 \[hep-ph\]](#).

- [7] Z. Liu, L.-T. Wang, and H. Zhang, *Exotic decays of the 125 GeV Higgs boson at future  $e^+e^-$  lepton colliders*, *Chin. Phys. C* **41** no. 6, (2017) 063102, [arXiv:1612.09284 \[hep-ph\]](#).
- [8] J. Gu, H. Li, Z. Liu, S. Su, and W. Su, *Learning from Higgs Physics at Future Higgs Factories*, *JHEP* **12** (2017) 153, [arXiv:1709.06103 \[hep-ph\]](#).
- [9] G. Durieux, C. Grojean, J. Gu, and K. Wang, *The leptonic future of the Higgs*, *JHEP* **09** (2017) 014, [arXiv:1704.02333 \[hep-ph\]](#).
- [10] T. Barklow, K. Fujii, S. Jung, R. Karl, J. List, T. Ogawa, M. E. Peskin, and J. Tian, *Improved Formalism for Precision Higgs Coupling Fits*, *Phys. Rev. D* **97** no. 5, (2018) 053003, [arXiv:1708.08912 \[hep-ph\]](#).
- [11] A. Voigt and S. Westhoff, *Virtual signatures of dark sectors in Higgs couplings*, *JHEP* **11** (2017) 009, [arXiv:1708.01614 \[hep-ph\]](#).
- [12] F. An *et al.*, *Precision Higgs physics at the CEPC*, *Chin. Phys. C* **43** no. 4, (2019) 043002, [arXiv:1810.09037 \[hep-ex\]](#).
- [13] R. Franceschini *et al.*, *The CLIC Potential for New Physics*, [arXiv:1812.02093 \[hep-ph\]](#).
- [14] J. De Blas, G. Durieux, C. Grojean, J. Gu, and A. Paul, *On the future of Higgs, electroweak and diboson measurements at lepton colliders*, *JHEP* **12** (2019) 117, [arXiv:1907.04311 \[hep-ph\]](#).
- [15] Y. Tan, X. Shi, R. Kiuchi, M. Ruan, M. Jing, X. Mo, X. Lou, G. Li, K. Zhang, and S. Jyotishmati, *Search for invisible decay of a Higgs boson produced at the CEPC*, [arXiv:2001.05912 \[hep-ex\]](#).
- [16] S. Jung, J. Lee, M. Perelló, J. Tian, and M. Vos, *Higgs, top and electro-weak precision measurements at future  $e^+e^-$  colliders; a combined effective field theory analysis with renormalization mixing*, [arXiv:2006.14631 \[hep-ph\]](#).
- [17] E. Fuchs, O. Matsedonskyi, I. Savoray, and M. Schlaffer, *Collider searches of scalar singlets across lifetimes*, [arXiv:2008.12773 \[hep-ph\]](#).
- [18] H. Li, H. Song, S. Su, W. Su, and J. M. Yang, *MSSM at future Higgs factories*, [arXiv:2010.09782 \[hep-ph\]](#).
- [19] P. Drechsel, G. Moortgat-Pick, and G. Weiglein, *Prospects for direct searches for light Higgs bosons at the ILC with 250 GeV*, *Eur. Phys. J. C* **80** no. 10, (2020) 922, [arXiv:1801.09662 \[hep-ph\]](#).
- [20] J. Kalinowski, W. Kotlarski, T. Robens, D. Sokolowska, and A. F. Zarnecki, *Exploring Inert*



- Scalars at CLIC*, *JHEP* **07** (2019) 053, [arXiv:1811.06952](#) [hep-ph].
- [21] H. Bahl, P. Bechtle, S. Heinemeyer, S. Liebler, T. Stefaniak, and G. Weiglein, *HL-LHC and ILC sensitivities in the hunt for heavy Higgs bosons*, *Eur. Phys. J. C* **80** no. 10, (2020) 916, [arXiv:2005.14536](#) [hep-ph].
- [22] **CEPC Study Group** Collaboration, *CEPC Conceptual Design Report: Volume 1 - Accelerator*, [arXiv:1809.00285](#) [physics.acc-ph].
- [23] J. a. B. Guimarães da Costa *et al.*, , **CEPC Study Group Collaboration** Collaboration, *CEPC Conceptual Design Report: Volume 2 - Physics & Detector*, tech. rep., Nov, 2018. [arXiv:1811.10545](#) [hep-ex]. 424 pages.
- [24] *The International Linear Collider Technical Design Report - Volume 1: Executive Summary*, [arXiv:1306.6327](#) [physics.acc-ph].
- [25] *The International Linear Collider Technical Design Report - Volume 2: Physics*, [arXiv:1306.6352](#) [hep-ph].
- [26] *The International Linear Collider Technical Design Report - Volume 3.I: Accelerator & in the Technical Design Phase*, [arXiv:1306.6353](#) [physics.acc-ph].
- [27] A. Abada *et al.*, , **FCC** Collaboration, *FCC-ee: The Lepton Collider: Future Circular Collider Conceptual Design Report Volume 2*, *Eur. Phys. J. ST* **228** no. 2, (2019) 261–623.
- [28] P. Langacker, *The Physics of Heavy  $Z'$  Gauge Bosons*, *Rev. Mod. Phys.* **81** (2009) 1199–1228, [arXiv:0801.1345](#) [hep-ph].
- [29] J. Jaeckel and A. Ringwald, *The Low-Energy Frontier of Particle Physics*, *Ann. Rev. Nucl. Part. Sci.* **60** (2010) 405–437, [arXiv:1002.0329](#) [hep-ph].
- [30] *Fundamental Physics at the Intensity Frontier*. 5, 2012. [arXiv:1205.2671](#) [hep-ex].
- [31] R. Essig *et al.*, *Working Group Report: New Light Weakly Coupled Particles*, in *Community Summer Study 2013: Snowmass on the Mississippi*. 10, 2013. [arXiv:1311.0029](#) [hep-ph].
- [32] J. Alexander *et al.*, *Dark Sectors 2016 Workshop: Community Report*, 8, 2016. [arXiv:1608.08632](#) [hep-ph].
- [33] M. Battaglieri *et al.*, *US Cosmic Visions: New Ideas in Dark Matter 2017: Community Report*, in *U.S. Cosmic Visions: New Ideas in Dark Matter*. 7, 2017. [arXiv:1707.04591](#) [hep-ph].
- [34] B. Holdom, *Two  $U(1)$ 's and Epsilon Charge Shifts*, *Phys. Lett. B* **166** (1986) 196–198.
- [35] P. Galison and A. Manohar, *TWO  $Z$ 's OR NOT TWO  $Z$ 's?*, *Phys. Lett. B* **136** (1984)

279–283.

- [36] K. R. Dienes, C. F. Kolda, and J. March-Russell, *Kinetic mixing and the supersymmetric gauge hierarchy*, *Nucl. Phys. B* **492** (1997) 104–118, [arXiv:hep-ph/9610479](#).
- [37] J. D. Bjorken, R. Essig, P. Schuster, and N. Toro, *New Fixed-Target Experiments to Search for Dark Gauge Forces*, *Phys. Rev. D* **80** (2009) 075018, [arXiv:0906.0580 \[hep-ph\]](#).
- [38] H. Davoudiasl, H.-S. Lee, and W. J. Marciano, *Muon Anomaly and Dark Parity Violation*, *Phys. Rev. Lett.* **109** (2012) 031802, [arXiv:1205.2709 \[hep-ph\]](#).
- [39] H. Davoudiasl, H.-S. Lee, I. Lewis, and W. J. Marciano, *Higgs Decays as a Window into the Dark Sector*, *Phys. Rev. D* **88** no. 1, (2013) 015022, [arXiv:1304.4935 \[hep-ph\]](#).
- [40] H. Davoudiasl, H.-S. Lee, and W. J. Marciano, *'Dark' Z implications for Parity Violation, Rare Meson Decays, and Higgs Physics*, *Phys. Rev. D* **85** (2012) 115019, [arXiv:1203.2947 \[hep-ph\]](#).
- [41] H. Davoudiasl, H.-S. Lee, and W. J. Marciano, *Low  $Q^2$  weak mixing angle measurements and rare Higgs decays*, *Phys. Rev. D* **92** no. 5, (2015) 055005, [arXiv:1507.00352 \[hep-ph\]](#).
- [42] D. Curtin *et al.*, *Exotic decays of the 125 GeV Higgs boson*, *Phys. Rev. D* **90** no. 7, (2014) 075004, [arXiv:1312.4992 \[hep-ph\]](#).
- [43] D. Curtin, R. Essig, S. Gori, and J. Shelton, *Illuminating Dark Photons with High-Energy Colliders*, *JHEP* **02** (2015) 157, [arXiv:1412.0018 \[hep-ph\]](#).
- [44] S. Gopalakrishna, S. Jung, and J. D. Wells, *Higgs boson decays to four fermions through an abelian hidden sector*, *Phys. Rev. D* **78** (2008) 055002, [arXiv:0801.3456 \[hep-ph\]](#).
- [45] M. Aaboud *et al.*, , **ATLAS** Collaboration, *Search for Higgs boson decays to beyond-the-Standard-Model light bosons in four-lepton events with the ATLAS detector at  $\sqrt{s} = 13$  TeV*, *JHEP* **06** (2018) 166, [arXiv:1802.03388 \[hep-ex\]](#).
- [46] **CMS Collaboration** Collaboration, *Search for a low-mass dilepton resonance in Higgs boson decays to four-lepton final states at  $\sqrt{s} = 13$  TeV*, Tech. Rep. CMS-PAS-HIG-19-007, CERN, Geneva, 2020.
- [47] H. Davoudiasl, H.-S. Lee, and W. J. Marciano, *Dark Side of Higgs Diphoton Decays and Muon  $g-2$* , *Phys. Rev. D* **86** (2012) 095009, [arXiv:1208.2973 \[hep-ph\]](#).
- [48] H. Davoudiasl, H.-S. Lee, and W. J. Marciano, *Muon  $g - 2$ , rare kaon decays, and parity violation from dark bosons*, *Phys. Rev. D* **89** no. 9, (2014) 095006, [arXiv:1402.3620 \[hep-ph\]](#).

- [49] J. R. Andersen *et al.*, , **LHC Higgs Cross Section Working Group** Collaboration, *Handbook of LHC Higgs Cross Sections: 3. Higgs Properties*, arXiv:1307.1347 [hep-ph].
- [50] D. de Florian *et al.*, , **LHC Higgs Cross Section Working Group** Collaboration, *Handbook of LHC Higgs Cross Sections: 4. Deciphering the Nature of the Higgs Sector*, arXiv:1610.07922 [hep-ph].
- [51] J. Alwall, R. Frederix, S. Frixione, V. Hirschi, F. Maltoni, O. Mattelaer, H. S. Shao, T. Stelzer, P. Torrielli, and M. Zaro, *The automated computation of tree-level and next-to-leading order differential cross sections, and their matching to parton shower simulations*, *JHEP* **07** (2014) 079, arXiv:1405.0301 [hep-ph].
- [52] N. D. Christensen and C. Duhr, *FeynRules - Feynman rules made easy*, *Comput. Phys. Commun.* **180** (2009) 1614–1641, arXiv:0806.4194 [hep-ph].
- [53] A. Alloul, N. D. Christensen, C. Degrande, C. Duhr, and B. Fuks, *FeynRules 2.0 - A complete toolbox for tree-level phenomenology*, *Comput. Phys. Commun.* **185** (2014) 2250–2300, arXiv:1310.1921 [hep-ph].
- [54] G. Cowan, K. Cranmer, E. Gross, and O. Vitells, *Asymptotic formulae for likelihood-based tests of new physics*, *Eur. Phys. J. C* **71** (2011) 1554, arXiv:1007.1727 [physics.data-an]. [Erratum: *Eur.Phys.J.C* 73, 2501 (2013)].
- [55] **European Strategy Group** Collaboration, , *2020 Update of the European Strategy for Particle Physics*. CERN Council, Geneva, 2020.